

Targeted Nanoparticles Deliver siRNA to Melanoma

Yunching Chen¹, Surendar R. Bathula¹, Qi Yang¹ and Leaf Huang¹

Melanoma is a severe skin cancer that often leads to death. To examine the potential of small interfering RNA (siRNA) therapy for melanoma, we have developed anisamide-targeted nanoparticles that can systemically deliver siRNA into the cytoplasm of B16F10 murine melanoma cells, which express the sigma receptor. A c-Myc siRNA delivered by the targeted nanoparticles effectively suppressed c-Myc expression in the tumor and partially inhibited tumor growth. More significant tumor growth inhibition was observed with nanoparticles composed of *N,N*-distearyl-*N*-methyl-*N*-2-(*N'*-arginyl) aminoethyl ammonium chloride (DSAA), a guanidinium-containing cationic lipid, than with a commonly used cationic lipid, 1,2-dioleoyl-3-trimethylammonium-propane (DOTAP). Three daily injections of c-Myc siRNA formulated in the targeted nanoparticles containing DSAA could impair tumor growth, and the ED₅₀ of c-Myc siRNA was about 0.55 mg kg⁻¹. The targeted DSAA nanoparticles containing c-Myc siRNA sensitized B16F10 cells to paclitaxel (Taxol), resulting in a complete inhibition of tumor growth for 1 week. Treatments of c-Myc siRNA in the targeted nanoparticles containing DSAA also showed significant inhibition on the growth of MDA-MB-435 tumor. The enhanced anti-melanoma activity is probably related to the fact that DSAA, but not DOTAP, induced reactive oxygen species, triggered apoptosis, and downregulated antiapoptotic protein Bcl-2 in B16F10 melanoma cells. Thus, the targeted nanoparticles containing c-Myc siRNA may serve as an effective therapeutic agent for melanoma.

Journal of Investigative Dermatology (2010) **130**, 2790–2798; doi:10.1038/jid.2010.222; published online 5 August 2010

INTRODUCTION

Melanoma is the most serious type of skin cancer in the world, accounting for about 80% of deaths. Most patients develop metastases with the 5-year survival rate being only 14% (Sulaimon and Kitchell, 2003). Currently, improved therapeutic options such as chemotherapy and immunotherapy are increasing but the therapeutic outcome is still limited because of the resistance of melanoma cells to these agents (Atallah and Flaherty, 2005; Hersey, 2006; Zhang *et al.*, 2006). Most therapeutic agents trigger anticancer effects by induction of apoptosis or generation of reactive oxygen species (ROS; Hersey, 2006; Tuma, 2008). However, the best response rate produced by a single-agent chemotherapy or biochemotherapy for melanoma is only 16% (Atallah and

Flaherty, 2005; Tas *et al.*, 2005). There is still ample room for improvement in the treatment strategy (Mathieu *et al.*, 2007).

Overexpression of c-Myc has been found in more than half of human cancers (Nesbit *et al.*, 1999). More than 2,000 MYC-responsive genes have been identified. They are involved in cell cycle control, proliferation, cell death, cell adhesion, biosynthesis of ribosomal and transfer RNAs, protein synthesis, and metabolism (Dang *et al.*, 2006). In melanoma, c-Myc expression is essential for nucleotide metabolism and proliferation of tumor cells (Mannava *et al.*, 2008). Overexpression of c-Myc during progression of melanoma continuously suppresses oncogene-induced senescence in the cells (Zhuang *et al.*, 2008). In this study, we explored the possibility of small interfering RNA (siRNA) against c-Myc as a therapy for subcutaneous malignant melanoma in a syngeneic murine model and human xenograft tumor models (Hong *et al.*, 2006; Li *et al.*, 2008b).

siRNA therapy is a novel but potentially effective strategy for cancer treatment, with reduced toxicity compared with that commonly found with conventional cytotoxic drugs (Devi, 2006). Combination therapy using siRNA and one or more chemotherapy drugs may be beneficial in decreasing the required dose of the drug and improving the therapeutic effect. Downregulation of the epithelial growth factor receptor sensitizes small cell lung carcinoma to cisplatin, resulting in a significantly improved growth inhibition (Li *et al.*, 2008a). siRNA against *SLUG*, which is required for melanoma cell survival and metastasis progression, enhances the efficacy of cisplatin and fotemustine (Vannini *et al.*, 2007). siRNA-based therapy was also developed to treat melanoma (Amarzguioui *et al.*, 2006; Liu *et al.*, 2009;

¹Division of Molecular Pharmaceutics, Eshelman School of Pharmacy, University of North Carolina at Chapel Hill, Chapel Hill, North Carolina, USA

Correspondence: Leaf Huang, Division of Molecular Pharmaceutics, Eshelman School of Pharmacy, Campus Box 7360, Kerr Hall, University of North Carolina at Chapel Hill, Chapel Hill, North Carolina 27599, USA. E-mail: leafh@unc.edu

Abbreviations: DOTAP AA⁻, LPD nanoparticles containing DOTAP modified with PEG without any targeting ligand; DOTAP AA⁺, LPD nanoparticles containing DOTAP modified with PEG with an anisamide ligand; DSAA AA⁻, LPD nanoparticles containing DSAA modified with PEG without any targeting ligand; DOTAP, 1,2-dioleoyl-3-trimethylammonium-propane; DSAA AA⁺, LPD nanoparticles containing DSAA modified with PEG with an anisamide ligand; DSAA, *N,N*-distearyl-*N*-methyl-*N*-2-(*N'*-arginyl) aminoethyl ammonium chloride; LPD, liposome-polycation-DNA; PEG, polyethylene glycol; siRNA, small-interfering RNA; ROS, reactive oxygen species

Received 30 July 2009; revised 21 April 2010; accepted 11 June 2010; published online 5 August 2010

Villares *et al.*, 2008; Zamora-Avila *et al.*, 2009). For example, a combination of siRNAs against MDM2, c-Myc, and VEGF showed a tumor growth inhibition effect in the B16F10 melanoma lung metastasis model (Li *et al.*, 2008b). Systemic delivery of protease-activated receptor-1 siRNA significantly inhibited melanoma growth and metastasis (Villares *et al.*, 2008). Furthermore, STAT3 siRNA delivered with a lipid-substituted polyethylenimine induced apoptosis in B16 melanoma (Alshamsan *et al.*, 2010).

To increase the stability of siRNA in the blood and promote selective uptake of siRNA into the tumor cells, we have developed targeted liposome-polycation-DNA (LPD) nanoparticles containing cationic liposomes that are efficient at delivering siRNA to several different solid tumors in mouse models (Li *et al.*, 2008a, b). Here we show that a nanoparticle formulation targeted with anisamide, which binds with the sigma 1 receptor of melanoma cells, is effective in delivering siRNA to B16F10 melanoma in a murine syngeneic model. Furthermore, a cationic lipid *N,N*-distearyl-*N*-methyl-*N*-2-(*N*-arginyl) aminoethyl ammonium chloride (DSAA), which contains an arginine residue as the head group, was particularly suitable as a formulation lipid. Our study indicates that c-Myc siRNA, delivered by DSAA-containing nanoparticles, may affect different signaling pathways and sensitize the melanoma cells to chemotherapeutic agents such as paclitaxel. The nanoparticle formulation showed minimal immunotoxicity in normal mice.

RESULTS

Intracellular uptake of siRNA in B16F10 melanoma cells

We used anisamide-targeted LPD nanoparticles containing DSAA as a carrier lipid to specifically deliver siRNA to cultured B16F10 melanoma cells, which express the sigma receptor. The structure of DSAA is shown in Figure 1. The size of the nanoparticles was about 100 nm and the ζ potential was about 25 mV. To characterize the formulation, we used FITC-labeled siRNA to prepare targeted nanoparticles using DSAA as the cationic lipid. The final formulation was fractionated by Sepharose CL 2B column chromatography. Supplementary Figure S1 online indicates

that the amount of siRNA loaded into the final formulation was about 85% of the total siRNA. Because DSAA has not previously been reported, we compared the data collected with nanoparticles containing DSAA and with those containing a previously used lipid, 1,2-dioleoyl-3-trimethylammonium-propane (DOTAP). Table 1 summarizes the abbreviations used for the different formulations. As shown in Figure 2a, confocal microscopy showed that nanoparticles containing DSAA could deliver Cy-3-labeled siRNA into the cytoplasm of B16F10 cells more efficiently than those containing DOTAP. Furthermore, Cy-3 siRNA uptake by the cells treated with the targeted nanoparticles DSAA AA+ was much more efficient than that by cells treated with the nontargeted nanoparticles DSAA AA-. The results indicate that the nanoparticles containing DSAA could efficiently deliver siRNA into the tumor cells and the delivery was significantly enhanced by the presence of the targeting ligand (AA) on the nanoparticles.

Luciferase gene silencing *in vitro*

B16F10 cells stably transduced with the firefly luciferase gene were used to study *in vitro* gene silencing. The luciferase gene silencing effect of the nanoparticles containing DSAA was stronger than that of those containing DOTAP (Figure 2b).

Table 1. Abbreviations for the formulations used in the study

Abbreviation	Explanation
LPD	Liposome-polycation-DNA
DSAA AA+	LPD nanoparticles containing DSAA modified with PEG with an anisamide ligand
DSAA AA-	LPD nanoparticles containing DSAA modified with PEG without any targeting ligand
DOTAP AA+	LPD nanoparticles containing DOTAP modified with PEG with an anisamide ligand
DOTAP AA-	LPD nanoparticles containing DOTAP modified with PEG without any targeting ligand

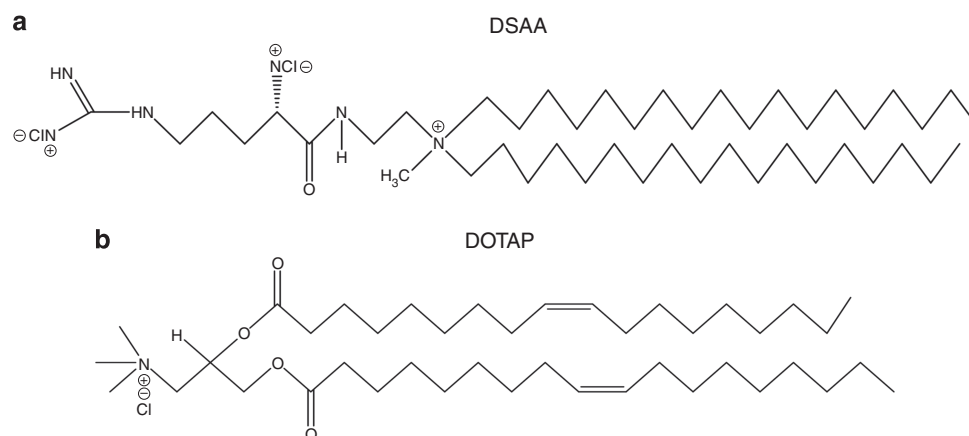


Figure 1. Chemical structures of DSAA and DOTAP. Chemical structures of DSAA (a) and DOTAP (b). DOTAP, 1,2-dioleoyl-3-trimethylammonium-propane; DSAA, *N,N*-distearyl-*N*-methyl-*N*-2-(*N*-arginyl) aminoethyl ammonium chloride.

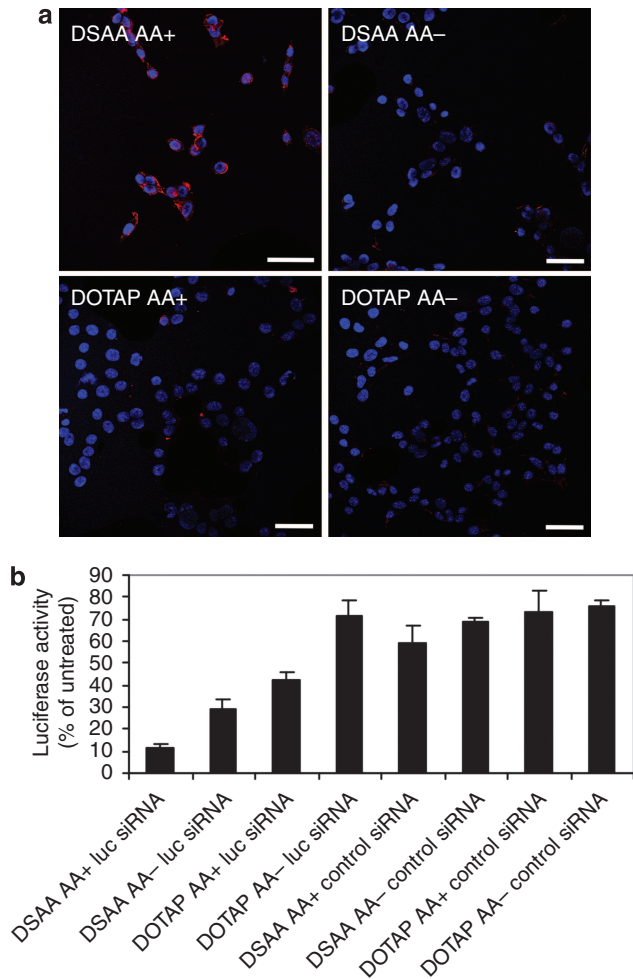


Figure 2. Intracellular uptake of siRNA and luciferase gene silencing in cultured melanoma cells. (a) Fluorescence micrographs of B16F10 cells after treatment with 5'-Cy-3-labeled siRNA in the targeted nanoparticles (AA+) or the nontargeted nanoparticles (AA-) containing DSAA and DOTAP. Scale bar = 50 μ m. (b) B16F10 cells were incubated with different formulations containing anti-luciferase siRNA. Luciferase activity in cells was measured after 24 hours. Each value represents the mean \pm SD ($n = 3$). DOTAP, 1,2-dioleoyl-3-trimethylammonium-propane; DSAA, *N,N*-distearyl-*N*-methyl-*N*-2-(*N*-arginyl) aminoethyl ammonium chloride; Luc, luciferase; siRNA, small interfering RNA.

Furthermore, the silencing effect in the cells treated with the targeted nanoparticles was much higher than that of cells treated with the nontargeted nanoparticles, when DSAA was the carrier lipid. The result correlated very well with that of the intracellular siRNA uptake (Figure 2a).

Tissue distribution and intracellular uptake of siRNA and lipid

We further studied the siRNA and lipid distribution and bioavailability of major tissues in the B16F10 melanoma model in C57BL/6 mice. We used 10 mol% 7-nitro-2-1,3-benzoxadiazol cholesterol-labeled liposomes (green) and Cy-3-labeled siRNA (red) to prepare PEGylated LPD and the final formulation was intravenously administered into the tumor-bearing mice. As shown in Figure 3a, a clear overlap (yellow/orange) between NBD-cholesterol-labeled liposomes and Cy-

3-labeled siRNA was observed, indicating intact nanoparticles were taken up by the tumor cells. The targeted nanoparticles containing DSAA or DOTAP (DSAA AA+ or DOTAP AA+) showed higher cytosolic delivery of Cy-3 siRNA and NBD cholesterol in the tumor tissue than the nontargeted nanoparticles (DSAA AA- or DOTAP AA-). Because the non-PEGylated liposomes containing DSAA/chol were a crucial component of the targeted nanoparticles (DSAA AA+), we compared the lipid (NBD cholesterol) uptake of DSAA AA+ with that of the non-PEGylated liposomes containing DSAA/chol. For quantitative results of lipid uptake (Figure 3b), the targeted nanoparticles containing DSAA showed higher lipid delivery in the tumor tissue than the non-PEGylated liposomes containing DSAA, whereas other tissues showed lower uptake of lipid when treated with the targeted nanoparticles containing DSAA than with the non-PEGylated liposome containing DSAA. Taken together, these data indicated that the targeted nanoparticles containing DSAA could efficiently deliver siRNA and the carrier lipid to the tumor tissue and the intracellular delivery was ligand dependent.

c-Myc gene silencing *in vivo*

To examine the biological activities of siRNA *in vivo*, we used western blotting to detect the *c-Myc* level in the subcutaneous melanoma tumor (Figure 4). *c-Myc* in B16F10 tumor was silenced by *c-Myc* siRNA in the targeted nanoparticles DSAA AA+ and DOTAP AA+. The *c-Myc* siRNA-containing DSAA AA- and DOTAP AA- and control siRNA showed no effect. The results of our study indicated that the nanoparticles containing DSAA or DOTAP could systemically deliver siRNA into the tumor tissue and that the delivery was specifically controlled by the targeting ligand (AA). The result correlated well with that of the intracellular siRNA uptake in the tumor tissue (Figure 3a).

Tumor growth inhibition

Three injections of *c-Myc* siRNA in DOTAP AA+ showed a partial inhibition of tumor growth ($P < 0.01$ at day 11) similar to that of *c-Myc* siRNA in DSAA AA- and control siRNA in DSAA AA+ (Figure 5a). A significant improvement in the tumor growth inhibition was observed with *c-Myc* siRNA formulated in DSAA AA+ ($P < 0.0001$ at day 11), with an ED_{50} of 0.55 mg kg^{-1} (Figure 5b). With additional treatment with paclitaxel, which is a common first-line chemotherapy agent for malignant melanoma, the therapeutic activity of *c-Myc* siRNA formulated in DSAA AA+ showed further improvement (Figure 5c). Tumor growth was completely inhibited by the combination therapy for 1 week after the last dose (Figure 5c).

Because DSAA was important in the uptake and the anticancer activity of siRNA delivered to the tumor cells, we decided to study the biological functions of DSAA in some detail. We first investigated the ROS activation in the B16F10 cells as it is important as an apoptosis inducer. B16F10 cells were treated with DOTAP/chol or DSAA/chol liposomes at different doses, and the cellular ROS content was measured by using 2',7'-dichlorodihydrofluorescein diacetate and flow cytometry. As shown in Figure 6, DSAA could generate ROS

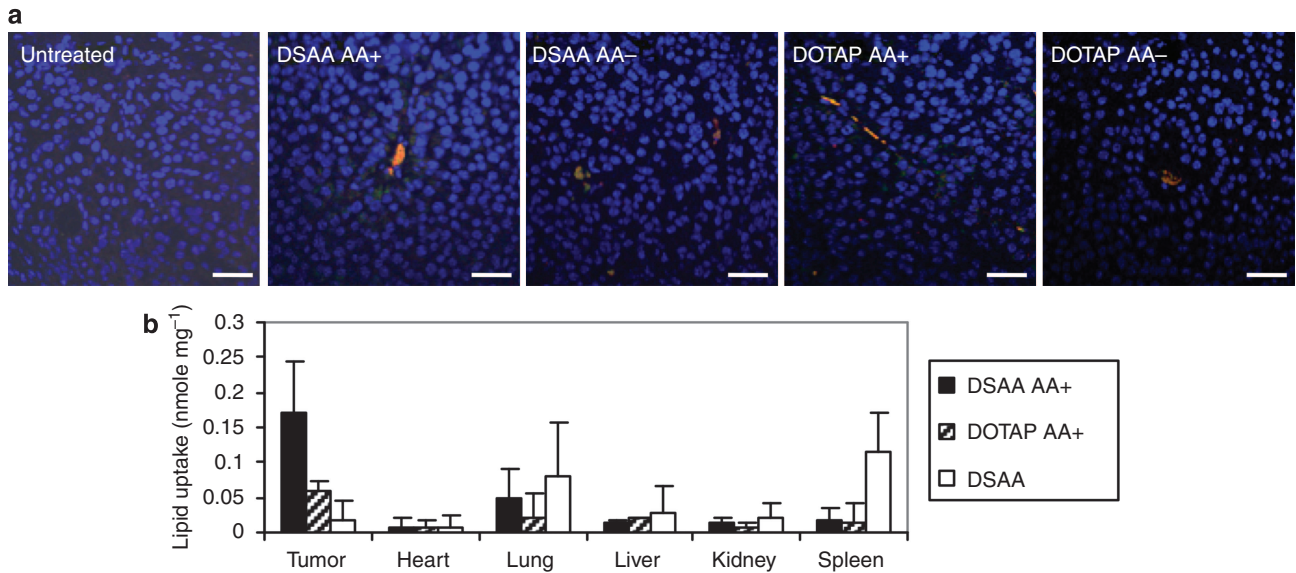


Figure 3. Tumor uptake of siRNA and lipid in different formulations. (a) Fluorescence micrographs of Cy-3-siRNA (red) and NBD-cholesterol (green) in B16F10 tumor. Mice were injected with different formulations and killed at 4 hours. Scale bar = 50 μ m. (b) Tissue distribution of NBD-cholesterol in mice injected with different formulations. Data = mean \pm SD, $n = 3$. DSAA: non-PEGylated liposome containing DSAA and cholesterol (1:1 mol ratio); siRNA, small interfering RNA.

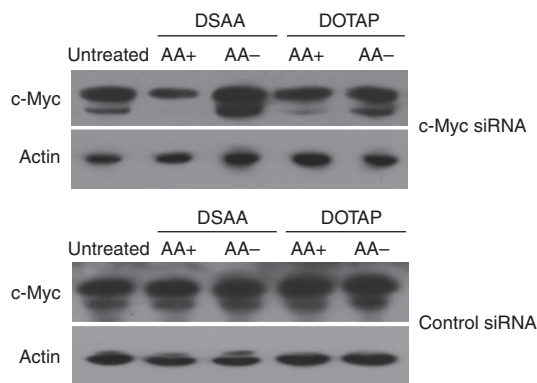


Figure 4. c-Myc expression in the tumor after treatment with siRNA in different formulations. Mice bearing B16F10 tumors were injected intravenously with siRNA formulated in different LPD nanoparticles. c-Myc expression was examined by western blot analysis. LPD, liposome-polycation-DNA; siRNA, small interfering RNA.

in B16F10 cells more efficiently than DOTAP after 1 hour of treatment, and the ROS induction was elevated in a dose-dependent manner. There was a statistically significant difference in the apoptosis induction between DSAA and DOTAP at concentrations of 10, 25, and 50 μ M after 24-hour incubation based on flow cytometry assay using propidium iodide and Annexin V staining (Figure 6b and c). Because it has been reported that ROS-induced apoptosis was regulated by the ubiquitination of Bcl-2 family proteins (Li *et al.*, 2004), we further studied the Bcl-2 protein expression after treatment of DSAA or DOTAP liposomes for different time periods in B16F10 cells. As shown in Figure 6d, 50 μ M DSAA could decrease Bcl-2 expression at 24 and 48 hours after treatment. However, Bcl-2 expression remained unchanged after the treatment with DOTAP. These results suggest that

ROS induced by DSAA may lead to apoptosis through Bcl-2 downregulation. Thus, silencing c-Myc by siRNA and ROS induction and the associated Bcl-2 downregulation by DSAA may work together to impair the growth of a melanoma tumor.

c-Myc gene silencing, apoptosis induction, and tumor growth inhibition in human melanoma

To further evaluate the clinical potential of c-Myc siRNA delivered by the targeted nanoparticles in human melanoma, we investigated the apoptosis induction and growth inhibition effects using the MDA-MB-435 human melanoma cell line (Rae *et al.*, 2007). We first determined the biological function of c-Myc siRNA on cell survival on MDA-MB-435 cells. Annexin V staining was carried out to detect apoptosis 72 hours after transfection. As shown in Figure 7a, apoptosis was significantly induced after the treatment with c-Myc siRNA compared with the control siRNA. To further evaluate apoptosis induction by c-Myc siRNA in the MDA-MB-435 xenograft model, we examined cellular apoptosis by using TUNEL staining (Figure 7b and c). As shown in the figure, c-Myc in MDA-MB-435 tumor was silenced by c-Myc siRNA in the targeted nanoparticles DSAA AA+. Control siRNA showed no effect. The number of TUNEL-positive cells increased after treatments of c-Myc delivered with the targeted nanoparticles DSAA AA+. Intravenous injections of control siRNA in the targeted nanoparticles DSAA AA+ showed a slight increase in TUNEL-positive cells. Five injections of c-Myc siRNA in the targeted nanoparticles DSAA AA+ showed significant inhibition of tumor growth ($P < 0.001$ at day 10). A partial tumor growth inhibition was observed with control siRNA formulated in DSAA AA+ ($P < 0.05$ at day 10; Figure 7d). These results suggested that c-Myc siRNA triggered apoptosis in MDA-MB-435 tumor and inhibited MDA-MB-435 melanoma growth.

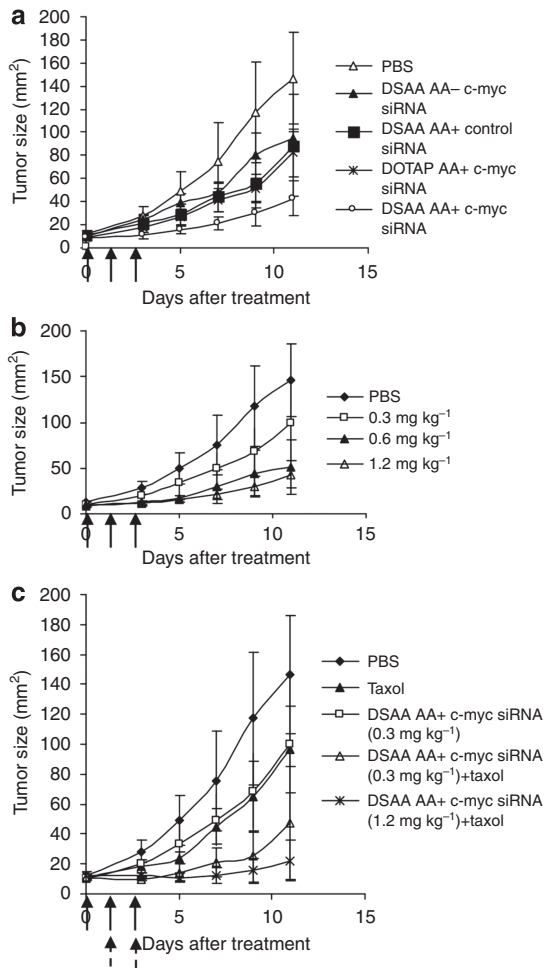


Figure 5. Tumor growth inhibition. (a) B16F10 tumor growth inhibition by siRNA in different formulations. (b) Dose-dependent antitumor activity of c-Myc siRNA formulated in DSAA AA+. (c) The combination of c-Myc siRNA formulated in the targeted DSAA nanoparticles and paclitaxel inhibited B16F10 tumor growth (20 mg paclitaxel per kg). Solid arrows indicate the i.v. administrations of siRNA, and dashed-line arrows indicate the i.v. injections of paclitaxel ($N = 4-7$). DSAA, *N,N*-distearyl-*N*-methyl-*N*-2-(*N*'-arginyl) aminoethyl ammonium chloride; siRNA, small interfering RNA.

Toxicity

The proinflammatory cytokine (IL-6 and IL-12) levels in the serum were examined for evaluation of immunotoxicity induced by our formulations in C57BL/6 mice (Supplementary Figure S2 online). c-Myc siRNA in different formulations (DSAA AA+, DSAA AA-, DOTAP AA+, and DOTAP AA-) induced a significant production of IL-12, whereas IL-6 was not induced by the formulations. Empty nanoparticles showed very mild immunotoxicity. When treated with lipopolysaccharide (1 mg kg^{-1}), both inflammatory cytokines were induced to high levels. The data suggested that the immunotoxicity of c-Myc siRNA in DSAA AA+ was similar to DOTAP AA+. Hepatotoxicity marker (aspartate aminotransferase and alanine aminotransferase) levels in the serum were examined for evaluation of toxicity induced by c-Myc siRNA in the target nanoparticles DSAA AA+ in C57BL/6 mice (Supplementary Table S1 online). Aspartate amino-

transferase and alanine aminotransferase levels remained the same as in the untreated animals. As DSAA significantly enhanced the anticancer activity, but not the toxicity, of c-Myc siRNA, it is a valuable formulation lipid for nanoparticles for the delivery of siRNA against melanoma.

DISCUSSION

Previous studies showed that a mixture of siRNAs against c-Myc, MDM2, and vascular endothelial growth factor had a tumor-inhibition effect on the B16F10 melanoma lung metastasis model (Li *et al.*, 2008b). In this study, we have improved the formulation by introducing a cationic lipid DSAA. Anisamide-targeted LPD nanoparticles containing DSAA effectively delivered siRNA to subcutaneous melanoma tumors and induced elevated apoptosis and tumor growth inhibition. Furthermore, c-Myc siRNA so delivered also sensitized the tumor cells to paclitaxel, a commonly used chemotherapeutic agent for malignant melanoma.

c-Myc oncoprotein, as a general transcription factor, regulates various key cellular processes such as cancer onset and maintenance in human tumors. Genetic aberrations of c-Myc promote tumorigenesis in various forms of cancer, leading to about 70,000 cancer deaths per year in the United States (Fest *et al.*, 2002). In melanoma, c-Myc expression and activation are also essential for cancer cell proliferation (Mannava *et al.*, 2008). Downregulation of c-Myc protein induces apoptosis in melanoma cells and sensitizes the tumor cells to anticancer drugs (Bucci *et al.*, 2005; Greco *et al.*, 2006). It has also been shown that overexpression of MYC oncoprotein inhibits apoptosis triggered by paclitaxel in human melanoma (Gatti *et al.*, 2009). Data presented in Figure 4 clearly indicate that c-Myc oncogene in the murine melanoma model could be effectively downregulated by using a systemic delivery vehicle carrying siRNA against c-Myc. Such downregulation brought tumor growth inhibition as predicted (Figure 5). The potency of this anti-melanoma treatment, as shown by the relatively low ED_{50} (0.55 mg kg^{-1} for siRNA), compares favorably with other siRNA-mediated therapies for cancer (Sonoke *et al.*, 2008). The therapy activity could be further enhanced by combining it with a commonly used first-line chemotherapy agent, i.e., paclitaxel.

A critical element for the success of the nanoparticle formulation is the cationic lipid DSAA. Our study data (Figure 6d) showed that the expression of Bcl-2 was downregulated in B16F10 melanoma cells after the treatment with DSAA. The reduction of Bcl-2 may be related to the induction of ROS in B16F10 cells by DSAA (Figure 6a). Bcl-2 is an antiapoptosis protein and overexpressed in various cancer cells. Downregulation of Bcl-2 renders the cancer cell more sensitive to cell death triggered by chemotherapeutic agents or radiation and leads to inhibition of tumor growth (Ciardiello and Tortora, 2002; Morris *et al.*, 2005). Chemotherapeutic drugs that promote downregulation of Bcl-2 trigger strong apoptotic activity in B16F10 cells (Jun *et al.*, 2007). c-Myc and Bcl-2 cooperate to suppress p53 functions in mediating chemotherapy-induced apoptosis (Evans *et al.*, 2006; Ryan *et al.*, 1994). Thus, it is not surprising that the combination of siRNA against c-Myc and DSAA downregulating Bcl-2 impaired the growth of the

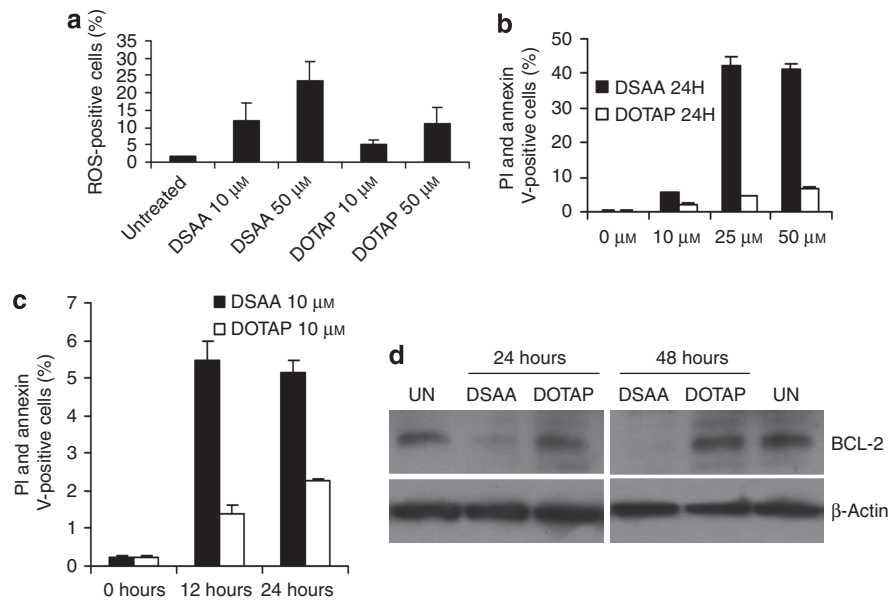


Figure 6. ROS generation and apoptosis induction by DSAA or DOTAP in mouse melanoma B16F10 cells. (a) Dose-dependent ROS generation by DSAA or DOTAP after 1 hour incubation with different concentrations of DSAA or DOTAP. The ROS content of cells was analyzed by flow cytometry. $N=3$, $*P<0.05$. (b and c) Dose- and time-dependent apoptosis induction by DSAA or DOTAP in B16F10 cells. (d) Bcl-2 expression in B16F10 cells after incubation with 50 μM DSAA and DOTAP for 24 and 48 hours. DOTAP, 1,2-dioleoyl-3-trimethylammonium-propane; DSAA, *N,N*-distearyl-*N*-methyl-*N*-2-(*N'*-arginyl) aminoethyl ammonium chloride; ROS, reactive oxygen species.

melanoma tumor and sensitized the tumor cells to paclitaxel. The combination therapy may also be considered for patients who develop drug resistance in tumors with overexpressed c-Myc. The possible mechanisms of the combination strategy using siRNA against c-Myc and DSAA are shown in Figure 8. DSAA induced ROS, triggered apoptosis, and downregulated antiapoptotic protein Bcl-2, which prevents the release of cytochrome *c* from mitochondria. c-Myc protein silencing by siRNA inhibited cell proliferation and sensitized melanoma cells to chemotherapy drugs. siRNA against c-Myc and DSAA may cooperate to activate nuclear translocation of p53 in mediating chemotherapy-induced apoptotic cell death in melanoma cells.

DSAA, a guanidinium-containing cationic lipid, induced ROS and triggered apoptosis in B16F10 melanoma cells in a dose- and time-dependent manner (Figure 6b and c). ROS have important functions affecting cell growth, death, development, and survival (Thannickal and Fanburg, 2000). Induction of ROS can initiate a lethal signal transduction resulting in damaged cellular integrity and apoptosis (Mates and Sanchez-Jimenez, 2000; Cejas *et al.*, 2004; Pelicano *et al.*, 2004; Lebedeva *et al.*, 2007). We suspected that the guanidinium residue had a critical function in the induction of ROS in the cells and that the generation of ROS collaborated with c-Myc siRNA to inhibit tumor growth. The activity of DOTAP in inducing ROS is very limited (Figure 6a) and hence had no effect in enhancing the tumor growth inhibition activity of c-Myc silencing (Figure 5a).

However, c-Myc is also involved in cell proliferation, cell growth, differentiation, and cell death in normal cells (Wierstra and Alves, 2008). In this study, we have used a targeted nanoparticle formulation (DSAA AA+) that can

specifically deliver c-Myc siRNA into tumor tissue (Figure 3a). Furthermore, the enhanced uptake of lipid into the tumor also appeared to be ligand dependent. The formulation was thus not very immunotoxic as shown in Supplementary Figure S1 online.

In summary, c-Myc siRNA formulated in the targeted nanoparticles containing DSAA could effectively impair tumor growth in the B16F10 melanoma model. The formulation shows great promise as an effective therapeutic agent, perhaps used together with some traditional chemotherapies, such as paclitaxel, for malignant melanoma.

MATERIALS AND METHODS

Materials

DOTAP and cholesterol were purchased from Avanti Polar Lipids (Alabaster, AL). Protamine sulfate and calf thymus DNA were from Sigma-Aldrich (St Louis, MO). Paclitaxel (Taxol) was purchased from Bristol-Myers Squibb (New York, NY). Synthetic 19-nt RNAs with 3' dTdT overhangs on both sequences were purchased from Dharmacon (Lafayette, CO). For quantitative studies, Cy-3 was conjugated to a 5' sense sequence. 5'-Cy-3-labeled siRNA sequence was also obtained from Dharmacon. The sequence of the mouse c-Myc siRNA was 5'-GAACAUCAUCAUCCAGGAC-3'. The sequence of the human c-Myc siRNA was 5'-AACGUUAGCUUCACCAACAUU-3' and the control siRNA with sequence 5'-AATTCTCCGAACGTGT CACGT-3' was obtained from Dharmacon. DSPE-PEG₂₀₀₀-anamide was synthesized in our laboratory using the methods described earlier (Banerjee *et al.*, 2004).

Cell culture

Murine melanoma B16F10 and human melanoma MDA-MB-435 (sigma receptor positive; Li *et al.*, 2008b) cells were used in this

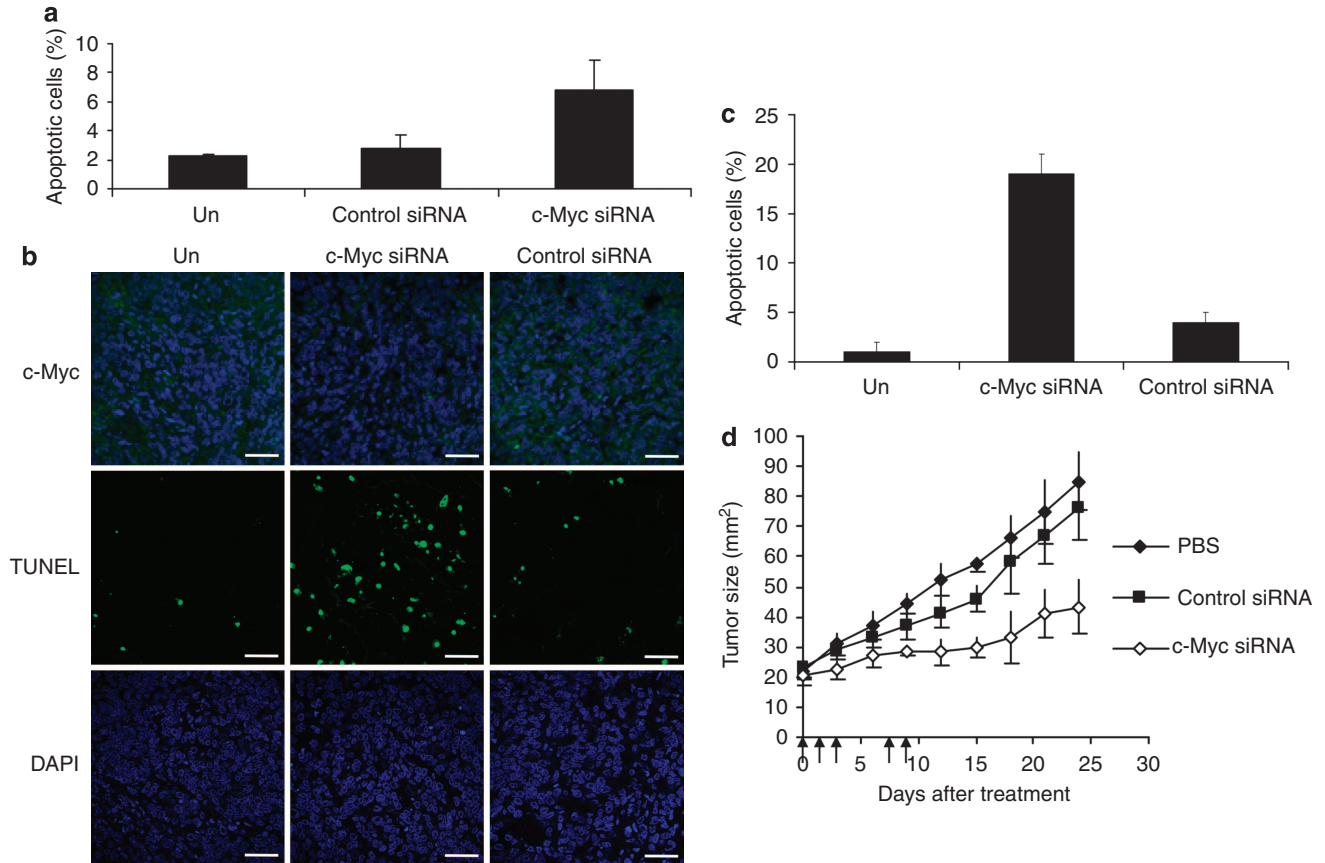


Figure 7. Apoptosis induction and tumor growth inhibition of human melanoma by nanoparticles containing c-Myc siRNA and DSAA. (a) MDA-MB-435 cells transfected with c-Myc or a control siRNA for 72 hours by lipofectamine 2000 and analyzed for Annexin V staining by flow cytometry. (b) Immunofluorescent staining of c-Myc and TUNEL staining in the MDA-MB-435 xenograft tumors after three consecutive i.v. injections of RNAs in targeted nanoparticles DSAA AA+. Scale bar = 50 μm . (c) Quantitative analysis of TUNEL-positive staining in the tumors treated with different formulations ($n = 3-6$). (d) Comparison of therapeutic efficacy of c-Myc (0.6 mg kg^{-1}) and control siRNAs in the targeted nanoparticles DSAA AA+. Arrows indicate the i.v. administrations of siRNA. DSAA, *N,N*-distearyl-*N*-methyl-*N*-2-(*N*-arginyl) aminoethyl ammonium chloride; DSASS, *N,N*-distearyl-*N*-methyl-*N*-2-(*N*-arginyl) aminoethyl ammonium chloride; siRNA, small interfering RNA.

study. The cells were purchased from the American Type Culture Collection. B16F10 cells were stably transduced with *GL3* firefly luciferase gene by using a retroviral vector produced in Pilar Blancafort's laboratory at the University of North Carolina at Chapel Hill. The cells were maintained in DMEM (Invitrogen, Carlsbad, CA) supplemented with 10% fetal bovine serum (Invitrogen), 100 U ml^{-1} penicillin, and $100 \mu\text{g ml}^{-1}$ streptomycin (Invitrogen).

Experimental animals

Female C57BL/6 mice 6-8 weeks of age were purchased from the National Cancer Institute (Frederick, MD). All work performed on animals was in accordance with and approved by the IACUC committee at UNC.

Synthesis of DSAA

DSAA is a non-glycerol-based guanidine head group containing cationic lipid synthesized in five steps. The synthesis is fairly simple. *N*-alkylation by *n*-octadecyl bromide and subsequent Boc deprotection of mono-Boc-protected ethylene diamine yielded mixed primary tertiary amine N^1, N^1 -dioctadecylethane-1,2-diamine. Tri-Boc-protected arginine conjugation to the primary amine group by the conventional EDCI and quaternization of the tertiary amine

group using methyl iodide on the above obtained product gave tri-Boc-protected DSAA. To obtain the final product DSAA, we carried out (*N*-2-(arginyl)ethyl)-*N*-methyl-*N,N*-dioctadecyl ammonium chloride) Boc group deprotection with TFA and chloride ion exchange with Amberlyst A 27 (Cl^-) ion exchange resin. The resulting compound was characterized by using ^1H NMR spectra and liquid secondary ion mass spectra. Detailed synthetic procedures and spectral and purity data will be delineated elsewhere (Bathula *et al.*, unpublished data).

Analysis of ROS in B16F10 cells

B16F10 cells (1×10^6 per well) were seeded into 12-well plates. Cells were incubated with 20 mM 2',7'-dichlorodihydrofluorescein diacetate (Sigma-Aldrich) in serum-containing medium for 30 minutes at 37°C . Then, cells were treated with DSAA or DOTAP liposomes at various doses in serum-containing medium at 37°C for 1 hour. Cells were quickly washed and immediately analyzed by flow cytometry.

Preparation of PEGylated LPD formulations

LPD were prepared according to the previously reported method with slight modifications (Cui *et al.*, 2005). Briefly, cationic

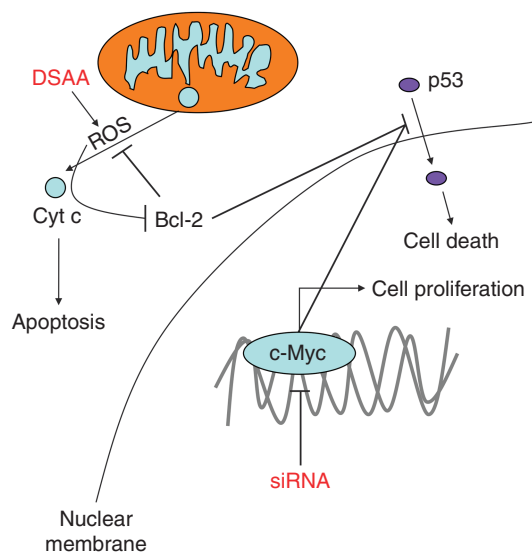


Figure 8. Schematic illustration of possible mechanisms of the combination strategy using c-Myc siRNA and the cationic lipid DSAA. Cyt c, cytochrome c; DSAA, *N,N*-distearyl-*N*-methyl-*N*-2-(*N*-arginyl) aminoethyl ammonium chloride; siRNA, small interfering RNA.

liposomes composed of DOTAP or DSAA and cholesterol (1:1 molar ratio) were prepared by thin film hydration followed by membrane extrusion to reduce the particle size. To prepare LPD, we mixed 18 μ l of protamine (2 mg ml⁻¹), 140 μ l of deionized water, and 24 μ l of a mixture of siRNA and calf thymus DNA (2 mg ml⁻¹) and kept it at room temperature for 10 minutes before adding 120 μ l of cationic liposome (10 mM). After 10 minutes at room temperature, LPD was mixed with 37.8 μ l of DSPE-PEG-AA or DSPE-PEG (10 mg ml⁻¹) and incubated at 50–60 °C for 10 minutes.

Cellular uptake study

B16F10 cells were seeded in 12-well plates (Corning, Corning, NY) 12 hours before experiments. Cells were treated with different formulations at a concentration of 250 nM for 5'-Cy-3-labeled siRNA in serum-containing medium at 37 °C for 4 hours. Cells were washed twice with phosphate-buffered saline, counterstained with 4,6-diamidino-2-phenyl indole, and imaged by using a Leica (Bannockburn, IL) SP2 confocal microscope.

Western blot analysis

For *in vivo* study, B16F10 tumor-bearing mice (tumor size \sim 1 cm²) were injected with siRNA in different formulations through the tail vein (1.2 mg siRNA per kg) with one injection per day for 3 consecutive days. The day after the third injection, mice were killed and tumor samples were collected. Extracted protein (40 μ g) from the tumor was separated on a 10% acrylamide gel and transferred to a polyvinylidene difluoride membrane. Membranes were blocked for 1 hour in 5% skim milk and then incubated for 12 hours with polyclonal antibodies directed against c-Myc (Santa Cruz Biotechnology) and actin (Santa Cruz Biotechnology) for standardization. Membranes were washed in PBST (phosphate-buffered saline, 0.1% Tween-20) and then incubated for 1 hour with appropriate secondary antibodies. Membranes were again washed and then developed by an enhanced chemiluminescence system according to the manufacturer's instructions (PerkinElmer, Covina, CA).

For *in vitro* Bcl-2 downregulation study, B16F10 cells were seeded in 12-well plates (1×10^5 per well) for 24 hours. Cells were treated with different lipids at the concentration of 50 μ M and were collected after 24 and 48 hours for measuring Bcl-2 expression by western blot analysis as described above.

Tumor uptake study

Mice with tumors \sim 1 cm² in size were injected intravenously with Cy-3-labeled siRNA (1.2 mg kg⁻¹) and NBD-labeled cholesterol (Avanti Polar Lipids) in different formulations. After 4 hours, mice were killed and tissues were collected, fixed in 10% formalin, and embedded in paraffin. Tumor tissues were sectioned ($7\frac{1}{4}$ μ m thick) and imaged using a Leica SP2 confocal microscope.

Tissue distribution study

Mice with tumors \sim 1 cm² in size were injected intravenously with NBD cholesterol in different formulations. After 4 hours, mice were killed and tissues were collected and homogenized in lysis buffer and incubated at room temperature for 30 minutes. The supernatant was collected after centrifugation at 14,000 r.p.m. for 10 minutes and 50 μ l supernatant was transferred to a black 96-well plate (Corning). The fluorescence intensity of the sample was measured by a plate reader (Bioscan, Washington, DC) at excitation wavelength 485 nm and emission wavelength 535 nm. Lipid concentration in each sample was calculated from a standard curve.

TUNEL assay

TUNEL staining was performed as recommended by the manufacturer (Promega, Madison, WI). MDA-MB-435 tumor-bearing mice were injected intravenously with siRNA formulated in the nanoparticles. At 24 hours after the third injection, the mice were killed and the tumors were collected for the TUNEL staining. Images from TUNEL-stained tumor sections were captured with Leica SP2 confocal microscopy.

Tumor growth inhibition study

B16F10 tumor-bearing mice (size 16–25 mm²) were injected intravenously with different formulations containing siRNA (1.2 mg kg⁻¹) once per day for 3 days. Tumor size in the treated mice was measured at different days after the treatment.

Analysis of serum cytokine levels

C57BL/6 mice were injected intravenously with siRNA against c-Myc in formulations at the dose of 1.2 mg siRNA per kg (1.2 mg DNA per kg for DSAA AA+ without siRNA). At 4 hours after the injections, blood samples were collected from the tail artery and allowed to stand on ice for 2 hours for coagulation. Serum was obtained by centrifuging the clotted blood at 16,000 r.p.m. for 20 minutes. Cytokine levels were determined by using ELISA kits for IL-6 and IL-12 (BD Biosciences, San Diego, CA).

Liver enzyme assay

The C57BL/6 mice were injected intravenously with c-Myc siRNA (1.2 mg kg⁻¹) formulated in the targeted nanoparticles. At 24 hours after injections, serum samples were obtained and the liver enzyme (alanine aminotransferase, aspartate aminotransferase) levels were analyzed by Animal Clinical Chemistry and Gene Expression Laboratories, University of North Carolina.

Statistical analysis

All statistical analyses were performed using Student's *t*-test. Data were considered statistically significant when the *P*-value was <0.05.

CONFLICT OF INTEREST

The authors state no conflict of interest.

ACKNOWLEDGMENTS

We thank the Michael Hooker Microscopy Facility at UNC for the microscopy images. This research was supported by NIH grant CA129825.

SUPPLEMENTARY MATERIAL

Supplementary material is linked to the online version of the paper at <http://www.nature.com/jid>

REFERENCES

- Alshamsan A, Hamdy S, Samuel J *et al.* (2010) The induction of tumor apoptosis in B16 melanoma following STAT3 siRNA delivery with a lipid-substituted polyethylenimine. *Biomaterials* 31:1420–8
- Amarzguoui M, Peng Q, Wiiger MT *et al.* (2006) *Ex vivo* and *in vivo* delivery of anti-tissue factor short interfering RNA inhibits mouse pulmonary metastasis of B16 melanoma cells. *Clin Cancer Res* 12:4055–61
- Atallah E, Flaherty L (2005) Treatment of metastatic malignant melanoma. *Curr Treat Options Oncol* 6:185–93
- Banerjee R, Tyagi P, Li S *et al.* (2004) Anisamide-targeted stealth liposomes: a potent carrier for targeting doxorubicin to human prostate cancer cells. *Int J Cancer* 112:693–700
- Bucci B, D'Agnano I, Amendola D *et al.* (2005) Myc down-regulation sensitizes melanoma cells to radiotherapy by inhibiting MLH1 and MSH2 mismatch repair proteins. *Clin Cancer Res* 11:2756–67
- Cejas P, Casado E, Belda-Iniesta C *et al.* (2004) Implications of oxidative stress and cell membrane lipid peroxidation in human cancer (Spain). *Cancer Causes Control* 15:707–19
- Ciardello F, Tortora G (2002) Inhibition of bcl-2 as cancer therapy. *Ann Oncol* 13:501–2
- Cui Z, Han SJ, Vangasseri DP *et al.* (2005) Immunostimulation mechanism of LPD nanoparticle as a vaccine carrier. *Mol Pharm* 2:22–8
- Dang CV, O'Donnell KA, Zeller KI *et al.* (2006) The c-Myc target gene network. *Semin Cancer Biol* 16:253–64
- Devi GR (2006) siRNA-based approaches in cancer therapy. *Cancer Gene Ther* 13:819–29
- Evans C, Morrison I, Heriot AG *et al.* (2006) The correlation between colorectal cancer rates of proliferation and apoptosis and systemic cytokine levels; plus their influence upon survival. *Br J Cancer* 94:1412–9
- Fest T, Mougey V, Dalstein V *et al.* (2002) c-MYC overexpression in Ba/F3 cells simultaneously elicits genomic instability and apoptosis. *Oncogene* 21:2981–90
- Gatti G, Maresca G, Natoli M *et al.* (2009) MYC prevents apoptosis and enhances endoreduplication induced by paclitaxel. *PLoS One* 4:e5442
- Greco C, D'Agnano I, Vitelli G *et al.* (2006) c-MYC deregulation is involved in melphalan resistance of multiple myeloma: role of PDGF-BB. *Int J Immunopathol Pharmacol* 19:67–79
- Hersey P (2006) Apoptosis and melanoma: how new insights are effecting the development of new therapies for melanoma. *Curr Opin Oncol* 18:189–96
- Hong J, Zhao Y, Huang W (2006) Blocking c-myc and stat3 by *E. coli* expressed and enzyme digested siRNA in mouse melanoma. *Biochem Biophys Res Commun* 348:600–5
- Jun HS, Park T, Lee CK *et al.* (2007) Capsaicin induced apoptosis of B16-F10 melanoma cells through down-regulation of Bcl-2. *Food Chem Toxicol* 45:708–15
- Lebedeva IV, Washington I, Sarkar D *et al.* (2007) Strategy for reversing resistance to a single anticancer agent in human prostate and pancreatic carcinomas. *Proc Natl Acad Sci USA* 104:3484–9
- Li D, Ueta E, Kimura T *et al.* (2004) Reactive oxygen species (ROS) control the expression of Bcl-2 family proteins by regulating their phosphorylation and ubiquitination. *Cancer Sci* 95:644–50
- Li SD, Chen YC, Hackett MJ *et al.* (2008a) Tumor-targeted delivery of siRNA by self-assembled nanoparticles. *Mol Ther* 16:163–9
- Li SD, Chono S, Huang L (2008b) Efficient oncogene silencing and metastasis inhibition via systemic delivery of siRNA. *Mol Ther* 16:942–6
- Liu Y, Tao J, Li Y *et al.* (2009) Targeting hypoxia-inducible factor-1alpha with Tf-PEI-shRNA complex via transferrin receptor-mediated endocytosis inhibits melanoma growth. *Mol Ther* 17:269–77
- Mannava S, Grachtchouk V, Wheeler LJ *et al.* (2008) Direct role of nucleotide metabolism in C-MYC-dependent proliferation of melanoma cells. *Cell Cycle* 7:2392–400
- Mates JM, Sanchez-Jimenez FM (2000) Role of reactive oxygen species in apoptosis: implications for cancer therapy. *Int J Biochem Cell Biol* 32:157–70
- Mathieu V, Le Mercier M, De Neve N *et al.* (2007) Galectin-1 knockdown increases sensitivity to temozolomide in a B16F10 mouse metastatic melanoma model. *J Invest Dermatol* 127:2399–410
- Morris MJ, Cordon-Cardo C, Kelly WK *et al.* (2005) Safety and biologic activity of intravenous BCL-2 antisense oligonucleotide (G3139) and taxane chemotherapy in patients with advanced cancer. *Appl Immunohistochem Mol Morphol* 13:6–13
- Nesbit CE, Tersak JM, Prochownik EV (1999) MYC oncogenes and human neoplastic disease. *Oncogene* 18:3004–16
- Pelicano H, Carney D, Huang P (2004) ROS stress in cancer cells and therapeutic implications. *Drug Resist Updat* 7:97–110
- Rae JM, Creighton CJ, Meck JM *et al.* (2007) MDA-MB-435 cells are derived from M14 melanoma cells—a loss for breast cancer, but a boon for melanoma research. *Breast Cancer Res Treat* 104:13–9
- Ryan JJ, Prochownik E, Gottlieb CA *et al.* (1994) c-myc and bcl-2 modulate p53 function by altering p53 subcellular trafficking during the cell cycle. *Proc Natl Acad Sci USA* 91:5878–82
- Sonoke S, Ueda T, Fujiwara K *et al.* (2008) Tumor regression in mice by delivery of Bcl-2 small interfering RNA with pegylated cationic liposomes. *Cancer Res* 68:8843–51
- Sulaimon SS, Kitchell BE (2003) The basic biology of malignant melanoma: molecular mechanisms of disease progression and comparative aspects. *J Vet Intern Med* 17:760–72
- Tas F, Argon A, Camlica H *et al.* (2005) Temozolomide in combination with cisplatin in patients with metastatic melanoma: a phase II trial. *Melanoma Res* 15:543–8
- Thannickal VJ, Fanburg BL (2000) Reactive oxygen species in cell signaling. *Am J Physiol Lung Cell Mol Physiol* 279:L1005–28
- Tuma RS (2008) Reactive oxygen species may have antitumor activity in metastatic melanoma. *J Natl Cancer Inst* 100:11–2
- Vannini I, Bonafe M, Tesei A *et al.* (2007) Short interfering RNA directed against the SLUG gene increases cell death induction in human melanoma cell lines exposed to cisplatin and fotemustine. *Cell Oncol* 29:279–87
- Villares GJ, Zigler M, Wang H *et al.* (2008) Targeting melanoma growth and metastasis with systemic delivery of liposome-incorporated protease-activated receptor-1 small interfering RNA. *Cancer Res* 68:9078–86
- Wierstra I, Alves J (2008) The c-myc promoter: still MysterY and challenge. *Adv Cancer Res* 99:113–333
- Zamora-Avila DE, Zapata-Benavides P, Franco-Molina MA *et al.* (2009) WT1 gene silencing by aerosol delivery of PEI-RNAi complexes inhibits B16-F10 lung metastases growth. *Cancer Gene Ther* 16:892–9
- Zhang XD, Wu JJ, Gillespie S *et al.* (2006) Human melanoma cells selected for resistance to apoptosis by prolonged exposure to tumor necrosis factor-related apoptosis-inducing ligand are more vulnerable to necrotic cell death induced by cisplatin. *Clin Cancer Res* 12:1355–64
- Zhuang D, Mannava S, Grachtchouk V *et al.* (2008) C-MYC overexpression is required for continuous suppression of oncogene-induced senescence in melanoma cells. *Oncogene* 27:6623–34